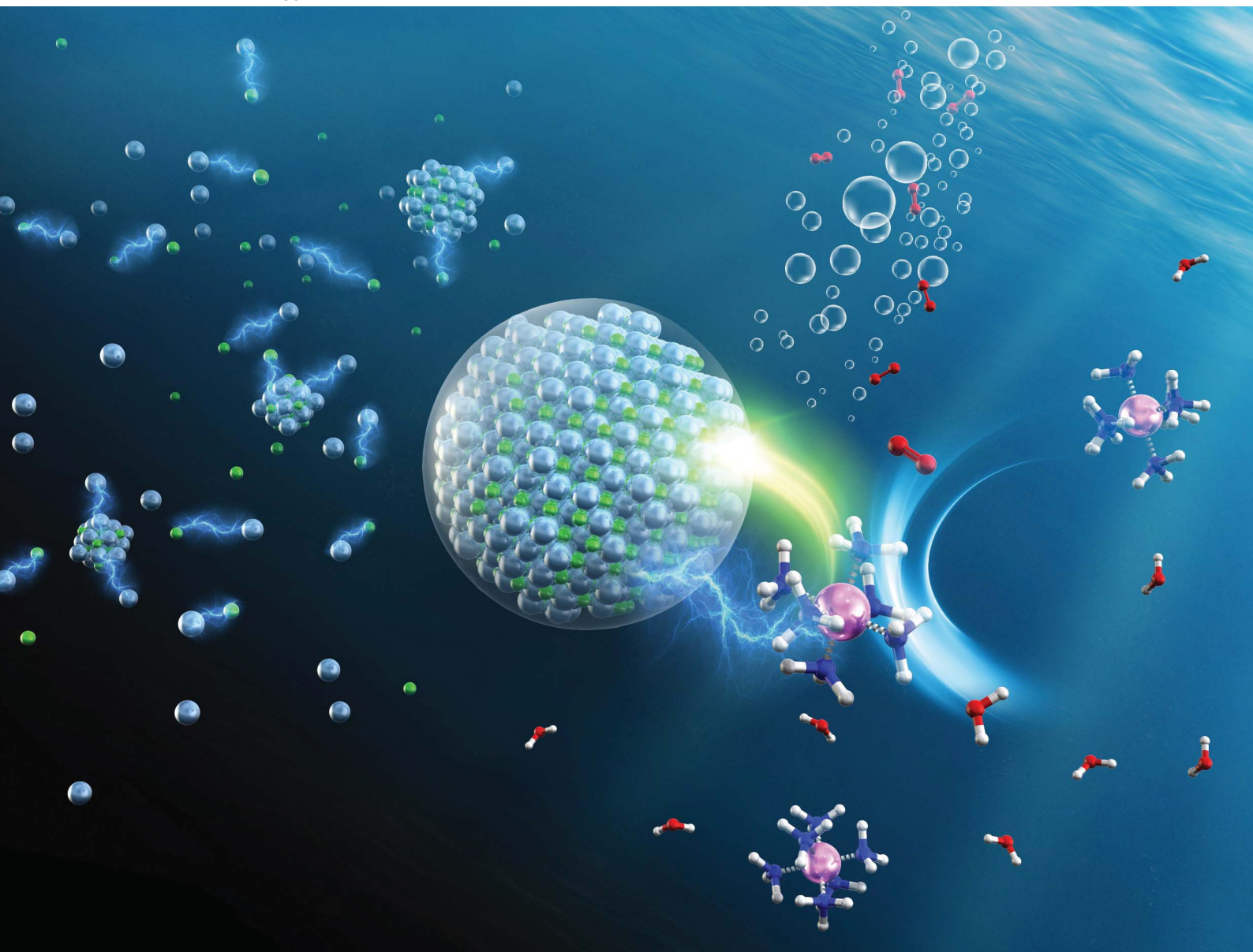


# Sustainable Energy & Fuels

Interdisciplinary research for the development of sustainable energy technologies

[rsc.li/sustainable-energy](https://rsc.li/sustainable-energy)



ISSN 2398-4902

**COMMUNICATION**

Kazuhiko Maeda *et al.*  
*In situ* formation of a molecular cobalt(III)/AgCl photocatalyst  
for visible-light water oxidation



Cite this: *Sustainable Energy Fuels*,  
2021, 5, 5694

Received 14th July 2021  
Accepted 31st August 2021

DOI: 10.1039/d1se01075a

rsc.li/sustainable-energy

Hexaamminecobalt(III) chloride underwent reaction in an aqueous  $\text{AgNO}_3$  solution containing a buffer base (pH 7–9), producing insoluble  $\text{AgCl}$  that showed no visible light photoresponse. The resultant molecular  $\text{Co(III)/AgCl}$  system showed water oxidation activity under visible light ( $\lambda > 400$  nm), approximately five times greater than that of a previously reported  $\text{CoO}_x/\text{anatase-TiO}_2$  photocatalyst.

Photocatalytic water splitting under irradiation with sunlight is an attractive solution to various energy and environmental issues.<sup>1–7</sup> Because  $\text{O}_2$  evolution requires the transfer of four electrons from two  $\text{H}_2\text{O}$  molecules, it is considered a difficult process from a kinetics perspective, hence necessitating a catalyst. Therefore, the development of a water oxidation catalyst (or photocatalyst) is an important research target in both heterogeneous and homogeneous systems,<sup>8–10</sup> even if a sacrificial electron acceptor is employed.<sup>11–16</sup>

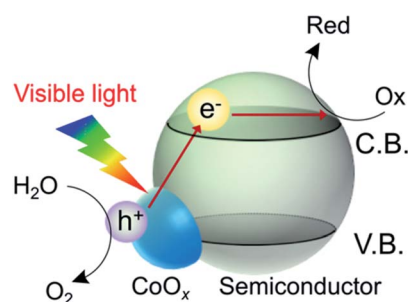
In metal (or metal oxide)/semiconductor composites, one may expect electron transitions from the loaded metal species to the conduction band of the semiconductor, and the metal-to-semiconductor electron transitions can be utilized for water oxidation photocatalysis.<sup>17–19</sup> Our group has reported that modifying a wide-bandgap semiconductor (e.g.,  $\text{TiO}_2$ ) with cobalt oxide ( $\text{CoO}_x$ ) or hydroxide ( $\text{Co(OH)}_2$ ) leads to the appearance of a new visible-light absorption band attributable to electron transitions from the loaded Co species to the conduction band of the semiconductor.<sup>20–22</sup> For example,  $\text{Co/TiO}_2$  hybrid materials are active as photocatalysts for water oxidation in the presence of  $\text{AgNO}_3$  as an electron acceptor under visible light, whereas unmodified  $\text{TiO}_2$  is inactive because

## *In situ* formation of a molecular cobalt(III)/AgCl photocatalyst for visible-light water oxidation†

Hiroto Mogi,<sup>a</sup> Megumi Okazaki,<sup>ab</sup> Shunta Nishioka<sup>a</sup> and Kazuhiko Maeda<sup>\*,a</sup>

of its large bandgap. We achieved  $\text{O}_2$  evolution even without physical contact between the Co species and the  $\text{TiO}_2$  support. Overall water splitting without a sacrificial reagent was also possible when  $\text{Co/TiO}_2$  was used as an anode in a photoelectrochemical cell.<sup>23</sup> Certain Co compounds are known to be good catalysts (or cocatalysts) for water oxidation.<sup>8–12,24,25</sup> Therefore, the Co species in these Co/semiconductor hybrid systems can be regarded as a “catalytic photosensitizer” for water oxidation (Scheme 1), which is unique in heterogeneous photocatalysis. However, the photocatalytic performance of the Co/semiconductor hybrid systems for water oxidation is still unsatisfactory, and the development of more active photocatalysts based on a catalytic Co photosensitizer is strongly desired.

In the present work, we report a new visible-light-driven water oxidation system based on a molecular  $\text{Co(III)}$  complex and a wide-gap semiconductor. We found that hexaamminecobalt(III) chloride ( $[\text{Co}(\text{NH}_3)_6]\text{Cl}_3$ ) undergoes reaction in an aqueous  $\text{AgNO}_3$  solution containing a buffer base (pH 7–9), producing a mixture of insoluble  $\text{AgCl}$  and aqueous  $[\text{Co}(\text{NH}_3)_6]^{3+}$  species. Surprisingly, the  $\text{Co(III)/AgCl}$  system, even



**Scheme 1** Water oxidation driven by charge transfer from a loaded Co species (e.g.,  $\text{CoO}_x$ ) to a semiconductor support. Even though the bandgap photoexcitation of the semiconductor from the valence band (V.B.) to the conduction band (C.B.) under visible light is not possible because of the large bandgap of the semiconductor, interfacial charge transfer from Co to the semiconductor may occur under visible light.

<sup>a</sup>Department of Chemistry, School of Science, Tokyo Institute of Technology, 2-12-1-NE-2 Ookayama, Meguro-ku, Tokyo 152-8550, Japan. E-mail: maedak@chem.titech.ac.jp

<sup>b</sup>Japan Society for the Promotion of Science, Kojimachi Business Center Building, 5-3-1 Kojimachi, Chiyoda-ku, Tokyo 102-0083, Japan

† Electronic supplementary information (ESI) available: Experimental details and additional characterization and photocatalytic reaction data. See DOI: 10.1039/d1se01075a



without any physical connection, exhibited approximately five-fold greater activity for visible-light water oxidation ( $\lambda > 400$  nm) compared with the activity of a previously reported  $\text{CoO}_x/\text{anatase-TiO}_2$  photocatalyst.

$[\text{Co}(\text{NH}_3)_6]^{3+}$  has previously been reported to function as a catalyst for water oxidation in the presence of  $[\text{Ru}(\text{bpy})_3]^{3+}$  as an oxidant.<sup>26</sup> The absorption spectrum of  $[\text{Co}(\text{NH}_3)_6]^{3+}$  shows a characteristic absorption band in the visible-light region (Fig. 1), which is assigned to d-d transitions ( $^1\text{A}_{1g} \rightarrow ^1\text{T}_{1g}$ ).  $\text{AgCl}$  has a cubic rocksalt structure and an indirect bandgap of 3.28 eV.<sup>27</sup> The absorption spectrum of our  $\text{AgCl}$  prepared *via* a precipitation reaction between  $\text{AgNO}_3$  and  $\text{HCl}$  (see the ESI† for details) showed an absorption edge at  $\sim 410$  nm (Fig. 1 and S1†), with an estimated bandgap of 3.0 eV, which is similar to the reported value. The spectrum of the as-prepared  $\text{AgCl}$  also showed an increased background in the visible-light region, presumably because of self-sensitization caused by reduced  $\text{Ag}$  species.<sup>28</sup> Although  $\text{AgCl}$  alone does not efficiently absorb visible light because of its large bandgap,  $\text{AgCl}$  modified with metals such as  $\text{Au}$  or  $\text{Ag}$  has been reported to act as a visible-light-driven “plasmonic” photocatalyst and/or photoanode.<sup>28–30</sup> However, the combination of  $\text{AgCl}$  with  $\text{Co}$  species for visible-light water oxidation has not yet been reported.

The water oxidation reaction was performed at room temperature using a top-irradiation-type reactor connected to a closed gas-circulation system.<sup>31</sup> The reaction solutions were prepared by adding different  $\text{Co}$  sources (*e.g.*,  $[\text{Co}(\text{NH}_3)_6]\text{Cl}_3$ ,  $\text{CoCl}_2$  and  $\text{Co}(\text{NO}_3)_2$ ) as “precatalysts” to a 5 mM  $\text{AgNO}_3$  solution (140 mL) containing 100 mg of  $\text{La}_2\text{O}_3$  as a pH buffering agent (pH  $\sim 8$ ).<sup>32</sup> After the reaction solution was degassed, irradiation was carried out using a 300 W Xe lamp and a cutoff filter. The evolved gases were analysed using an online gas chromatograph.

As shown in Fig. 2a, the  $[\text{Co}(\text{NH}_3)_6]\text{Cl}_3$  and  $\text{CoCl}_2$  systems produced  $\text{O}_2$  when irradiated with visible light ( $\lambda > 400$  nm), with initial rates of approximately 68 and 10  $\mu\text{mol h}^{-1}$ , respectively. By contrast, the use of  $\text{Co}(\text{NO}_3)_2$  did not yield  $\text{O}_2$ . Consequently, among the investigated precatalysts,  $[\text{Co}(\text{NH}_3)_6]\text{Cl}_3$  was determined to be the most appropriate for visible-light water oxidation. Under the optimal conditions, the activity of the  $[\text{Co}(\text{NH}_3)_6]\text{Cl}_3$  system was five times greater than that of the

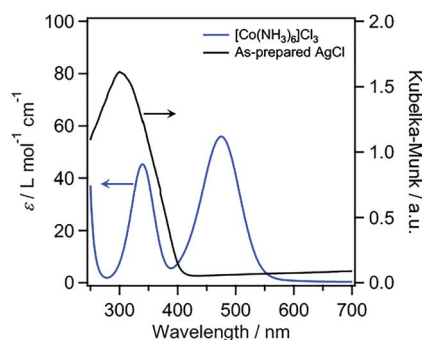


Fig. 1 UV-visible absorption spectrum of  $[\text{Co}(\text{NH}_3)_6]\text{Cl}_3$  (5 mM) in  $\text{H}_2\text{O}$  and the diffuse reflectance spectrum of the as-prepared  $\text{AgCl}$ .

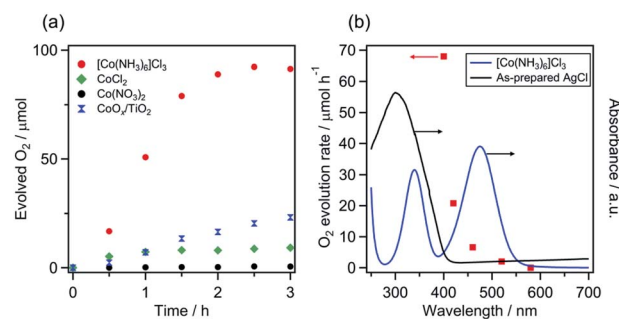


Fig. 2 (a) Time courses of  $\text{O}_2$  evolution over various precatalyst systems under visible light ( $\lambda > 400$  nm) and (b) the dependence of the rate of  $\text{O}_2$  evolution by the  $[\text{Co}(\text{NH}_3)_6]\text{Cl}_3$  system on the cutoff wavelength of incident light. Reaction conditions: precatalyst, 30 mg; 5 mM aqueous  $\text{AgNO}_3$  solution containing  $\text{La}_2\text{O}_3$  (100 mg), 140 mL; light source, 300 W Xe lamp with a CM-1 mirror and cutoff filter (L42, Y44, Y48, O54 or R60). In the case of the  $\text{CoO}_x/\text{TiO}_2$ : catalyst, 100 mg; 10 mM aqueous  $\text{AgNO}_3$  solution containing  $\text{La}_2\text{O}_3$  (200 mg). The actual time course data for the  $\text{O}_2$  evolution are shown in Fig. S6.†

photocatalyst  $\text{CoO}_x/\text{TiO}_2$ , which was previously reported to exhibit the highest activity among  $\text{Co}$ /wide-bandgap-semiconductor combinations.<sup>22</sup> The initial rate of  $\text{O}_2$  evolution over the  $[\text{Co}(\text{NH}_3)_6]\text{Cl}_3$  system was comparable to that recorded for representative visible-light-driven photocatalysts (*e.g.*,  $\text{TaON}$  and  $\text{LaTiO}_2\text{N}$ ),<sup>16</sup> which exhibited high water oxidation activities in aqueous  $\text{AgNO}_3$  solution with  $\text{La}_2\text{O}_3$ .

In the absence of  $\text{La}_2\text{O}_3$ , however, the  $\text{O}_2$  evolution activity of the  $[\text{Co}(\text{NH}_3)_6]\text{Cl}_3$  system decreased to almost 13% of its value when  $\text{La}_2\text{O}_3$  was present (Fig. S2†), which suggests that a pH of  $\sim 8$  is desirable for the efficient production of  $\text{O}_2$ . The effect of reaction pH on the  $\text{O}_2$  evolution activity was investigated in sodium tetraborate aqueous solutions without  $\text{La}_2\text{O}_3$ . As shown in Fig. S3,† relatively high  $\text{O}_2$  evolution rates were obtained at pH 7–9. However,  $\text{O}_2$  evolution was negligible above pH 10. At pH 10, it was found that the visible light absorption capability of  $[\text{Co}(\text{NH}_3)_6]\text{Cl}_3$  disappeared completely (Fig. S4†), which would be the main reason for the very low activity. These results again indicate the importance of reaction pH. Moreover, no  $\text{O}_2$  evolution was observed in the absence of either  $[\text{Co}(\text{NH}_3)_6]\text{Cl}_3$ ,  $\text{AgNO}_3$  or light irradiation. The fact that no  $\text{O}_2$  evolution was observed in the dark precludes a stoichiometric reaction between the high-valent  $[\text{Co}(\text{NH}_3)_6]\text{Cl}_3$  and  $\text{H}_2\text{O}$ . The apparent quantum yield of the  $[\text{Co}(\text{NH}_3)_6]\text{Cl}_3$  system was 0.20% under irradiation with 460 nm light (Fig. S5†).

Fig. 2b shows the dependence of the rate of  $\text{O}_2$  evolution by the  $[\text{Co}(\text{NH}_3)_6]\text{Cl}_3$  system on the wavelength of the incident light. The  $\text{O}_2$  evolution rate decreased with increasing wavelength of the incident light.  $\text{O}_2$  evolution was observable under irradiation with  $>520$  nm light but became almost zero under irradiation with  $>580$  nm light. The trend of  $\text{O}_2$  evolution appears to be associated with light absorption by  $[\text{Co}(\text{NH}_3)_6]\text{Cl}_3$ . However, the abrupt decrease observed when comparing the  $\text{O}_2$  evolution rate under  $\lambda > 400$  nm irradiation with that under  $\lambda > 420$  nm irradiation (Fig. 2b and S6†) strongly suggests that the activity is not simply correlated with the light-absorption





behaviour of  $[\text{Co}(\text{NH}_3)_6]\text{Cl}_3$ . These results will be discussed again in later sections.

Because the solubility product ( $K_{\text{sp}}$ ) of  $\text{AgCl}$  is  $1.8 \times 10^{-10} \text{ mol}^2 \text{ L}^{-2}$ ,<sup>33</sup>  $\text{AgCl}$  should be generated under the present reaction conditions, where 0.8 mM  $[\text{Co}(\text{NH}_3)_6]\text{Cl}_3$  and 5 mM  $\text{AgNO}_3$  coexist. The products obtained after photocatalytic reaction for 1 h, at which point the photocatalyst suspension exhibited sufficient activity to generate  $\text{O}_2$  (Fig. 2), were characterized by X-ray diffraction (XRD) and UV-visible spectroscopy measurements. As displayed in Fig. 3a, the XRD patterns show that the obtained product was a mixture of  $\text{La}(\text{OH})_3$ ,  $\text{AgCl}$  and  $\text{Ag}$ , with no peaks assignable to  $[\text{Co}(\text{NH}_3)_6]\text{Cl}_3$ . The production of  $\text{Ag}^0$ , as a result of the reduction of  $\text{Ag}^+$ , was also confirmed (Fig. S7†). Energy-dispersive X-ray spectroscopy analysis was conducted for the solid product; however, Co species were not measurable presumably because of the low concentration. These results strongly suggest that Co species existed predominantly in the solution phase under the investigated reaction conditions, and also preclude the possibility of Co nanoparticle formation. Fig. 3b shows the UV-visible absorption spectra of the reaction solution after filtration of the solid products. The peak intensity at 473 nm was almost unchanged after 1 h of reaction; however, a decrease in the intensity of the absorption at 340 nm ( $^1\text{A}_{1g} \rightarrow ^1\text{T}_{2g}$ ) was observed, along with the appearance of a new absorption band at  $\sim 300 \text{ nm}$ . The 300 nm-band is assigned to the absorption of  $\text{NO}_3^-$  species.<sup>34</sup> A substantial reduction of the

intensity of the visible-light absorption band was observed after 3 h of reaction, indicating the decomposition of  $[\text{Co}(\text{NH}_3)_6]^{3+}$ . This decomposition is likely one of the causes of photocatalyst deactivation, but the main cause of the deactivation is the consumption of  $\text{Ag}^+$  in the solution (see additional discussion in the ESI†).

On the basis of the aforementioned results, we concluded that the active photosystem consisted of aqueous  $[\text{Co}(\text{NH}_3)_6]^{3+}$  and  $\text{AgCl}$  as essential components. Note that approximately 0.36 mmol of  $\text{AgNO}_3$  still remain even if the formation of  $\text{AgCl}$  from  $[\text{Co}(\text{NH}_3)_6]\text{Cl}_3$  and  $\text{AgNO}_3$  in the initial reaction solution occurs stoichiometrically. Taken together, a possible reaction mechanism for  $\text{O}_2$  evolution by the  $[\text{Co}(\text{NH}_3)_6]\text{Cl}_3$  system is proposed (Scheme 2). Under dark conditions before irradiation,  $\text{AgCl}$  is formed by a reaction between  $[\text{Co}(\text{NH}_3)_6]\text{Cl}_3$  and  $\text{AgNO}_3$  in the reaction solution, as confirmed by XRD measurement (Fig. S1†). Visible-light irradiation of the suspension initiates electron transfer from water-soluble  $[\text{Co}(\text{NH}_3)_6]^{3+}$  species to the conduction band of  $\text{AgCl}$ , followed by the oxidation of water to  $\text{O}_2$  and the reduction of  $\text{Ag}^+$  to  $\text{Ag}$ , which occur on higher-valent (*i.e.*, electron-deficient) Co species and  $\text{AgCl}$ , respectively. It has been reported that the  $\zeta$ -potentials of a  $\text{AgCl}$  single crystal measured in aqueous  $\text{KNO}_3$  solution (1 and 10 mM) were negative at  $\text{pH} > 5$ .<sup>35</sup> This implies that there is an electrostatic attraction between the *in situ* formed  $\text{AgCl}$  and  $[\text{Co}(\text{NH}_3)_6]^{3+}$  species in the reactant solution, which benefits electron transfer from Co to  $\text{AgCl}$ . It appears, however, that the electrostatic attraction is too weak to bind  $[\text{Co}(\text{NH}_3)_6]^{3+}$  on the  $\text{AgCl}$  surface. Another possibility that  $[\text{Co}(\text{NH}_3)_6]^{3+}$  species undergo photoexcitation and then inject an electron into  $\text{AgCl}$  is not realistic because  $[\text{Co}(\text{NH}_3)_6]^{3+}$  is a non-emissive complex (*i.e.*, the lifetime of the photoexcited state is too short to induce a photoinduced electron transfer reaction from its excited state).

The presence of  $\text{AgCl}$  formed *in situ* in the reaction solution was found to be indispensable for obtaining a measurable amount of  $\text{O}_2$ . When  $\text{AgCl}$  particles were intentionally removed from the solution by filtration prior to photoreaction, the  $\text{O}_2$  evolution activity decreased substantially (black squares, Fig. S8†). This confirms that  $\text{AgCl}$  is essential for achieving visible-light water oxidation with  $[\text{Co}(\text{NH}_3)_6]^{3+}$ . When the homemade  $\text{AgCl}$  was added to the filtered (*i.e.*,  $\text{AgCl}$ -free) suspension and the photoreaction was conducted, a small amount of  $\text{O}_2$  evolution was observed (green diamonds). The addition of  $\text{NaCl}$  to the filtered suspension produced  $\text{AgCl}$

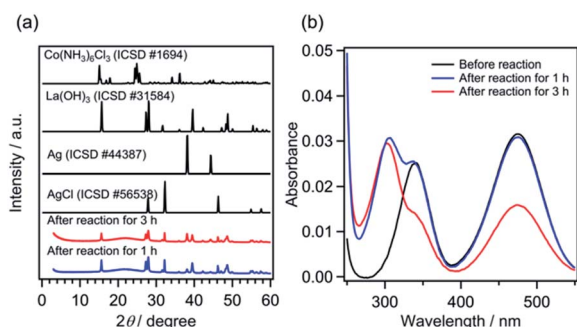
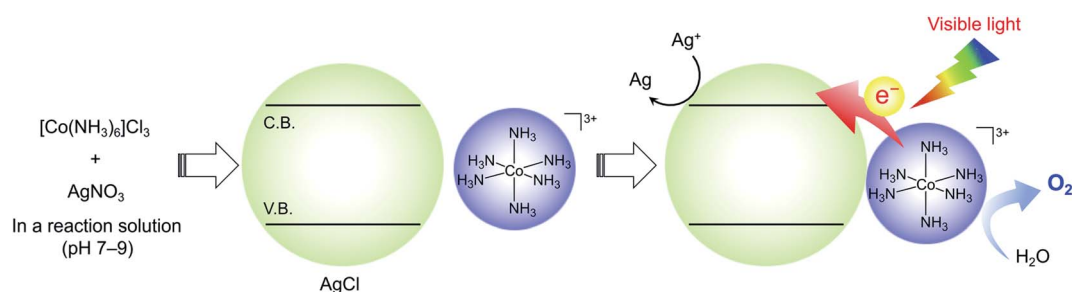


Fig. 3 (a) XRD patterns of the obtained products and (b) UV-visible absorption spectra of reaction solutions after different reaction times. The solution collected after filtration was diluted with  $\text{H}_2\text{O}$  to prepare a 200 mL solution for measurements. The sample "Before reaction" in panel (b) did not include  $\text{AgNO}_3$ , but only contained 0.56 mM  $[\text{Co}(\text{NH}_3)_6]\text{Cl}_3$ .



Scheme 2 Proposed reaction mechanism for visible-light-driven water oxidation over the  $[\text{Co}(\text{NH}_3)_6]^{3+}/\text{AgCl}$  system.



again, resulting in measurable O<sub>2</sub> evolution (green squares). However, the thus-obtained activities were much lower than the activity of the standard [Co(NH<sub>3</sub>)<sub>6</sub>]<sup>3+</sup>/AgCl suspension. As shown in Fig. 2a, the Co(NO<sub>3</sub>)<sub>2</sub> system produced negligible O<sub>2</sub>. However, the coexistence of NaCl in the Co(NO<sub>3</sub>)<sub>2</sub> system led to an improvement of the O<sub>2</sub> evolution rate to 14 μmol h<sup>-1</sup> (blue diamonds, Fig. S8†). In this case, AgCl formation by the reaction between NaCl and AgNO<sub>3</sub> was clearly indicated by naked-eye observation of a white precipitate in the solution. All these results indicate the importance of the *in situ*-generated AgCl, which plays a key role in oxidizing water to O<sub>2</sub> in the presence of Co species. Interestingly, O<sub>2</sub> evolution from a mixed system consisting of [Co(NH<sub>3</sub>)<sub>6</sub>]<sup>3+</sup> and TiO<sub>2</sub> was very slow, as compared to that recorded for the standard [Co(NH<sub>3</sub>)<sub>6</sub>]<sup>3+</sup>/AgCl system (Fig. S2†).

Notably, even in the presence of a Cl<sup>-</sup>-containing precatalyst that can form AgCl during the reaction, precatalysts with higher-valent Co (here [Co(NH<sub>3</sub>)<sub>6</sub>]Cl<sub>3</sub>) exhibited better performance (Fig. 2a). This result is likely attributable to the higher-valence metal species which are generally advantageous in water oxidation catalysis because of their strong oxidizing ability. Water oxidation in the presence of NaCl without a Co precatalyst hardly occurred as well (orange triangles, Fig. S8†). The AgCl formed by the reaction between NaCl and AgNO<sub>3</sub> showed a small absorption band in the visible region (Fig. S1†). However, it is clear that the visible light absorption of AgCl does not contribute to O<sub>2</sub> evolution. Therefore, if the direct photoexcitation of AgCl occurs at all, it is a minor reaction path during water oxidation by the [Co(NH<sub>3</sub>)<sub>6</sub>]Cl<sub>3</sub> system.

## Conclusions

In summary, we developed a new visible-light-driven water oxidation system that consists of *in situ*-formed AgCl and [Co(NH<sub>3</sub>)<sub>6</sub>]<sup>3+</sup>. Although AgCl and [Co(NH<sub>3</sub>)<sub>6</sub>]<sup>3+</sup> were individually almost inactive toward visible-light water oxidation, the combination of the two, even without distinct chemical bond linkage, yielded clear photocatalytic activity for water oxidation at pH 7–9 under visible-light irradiation; the activity was five times greater than that of a previously reported CoO<sub>x</sub>/anatase TiO<sub>2</sub> system. The results of the present study also suggest that the resultant photocatalytic activities were dependent on the valence state of the Co species initially employed, and that suitable combinations of a molecular catalyst and a semiconductor may give us more active photosystems.

It has been shown that in metal-complex/semiconductor hybrid photocatalysts for CO<sub>2</sub> reduction, electron transfer from suspended semiconductor particles to dissolved metal complexes can occur, even without any chemical bond linkage between the two components.<sup>36,37</sup> Therefore, the present water oxidation system is another example of the electron transfer type reaction between a molecule and a semiconductor. As mentioned, [Co(NH<sub>3</sub>)<sub>6</sub>]<sup>3+</sup> has been reported to act as a catalyst for water oxidation,<sup>26</sup> but is generally considered to be inactive for ligand exchange. Further investigations of the underlying mechanism and the development of other photocatalytic reactions using this strategy are underway in our laboratory.

## Author contributions

The manuscript was written with contributions from all authors. All authors have given approval to the final version of the manuscript.

## Conflicts of interest

There are no conflicts to declare.

## Acknowledgements

This work was supported by a Grant-in-Aid for Scientific Research (B) (Project JP19H02511). M. O. wishes to acknowledge support by a JSPS Fellowship for Young Scientists (JP19J21858).

## Notes and references

- 1 R. Abe, *Bull. Chem. Soc. Jpn.*, 2011, **84**, 1000–1030.
- 2 F. E. Osterloh, *Chem. Soc. Rev.*, 2013, **42**, 2294–2320.
- 3 Y. Ma, X. Wang, Y. Jia, X. Chen, H. Han and C. Li, *Chem. Rev.*, 2014, **114**, 9987–10043.
- 4 Y. Zheng, L. Lin, B. Wang and X. Wang, *Angew. Chem., Int. Ed.*, 2015, **54**, 12868–12884.
- 5 K. Maeda and K. Domen, *Bull. Chem. Soc. Jpn.*, 2016, **89**, 627–648.
- 6 K. Maeda and T. E. Mallouk, *Bull. Chem. Soc. Jpn.*, 2019, **92**, 38–54.
- 7 A. Miyoshi and K. Maeda, *Sol. RRL*, 2020, **5**, 2000521.
- 8 M. W. Kanan, Y. Surendranath and D. G. Nocera, *Chem. Soc. Rev.*, 2009, **38**, 109–114.
- 9 F. Jiao and H. Frei, *Energy Environ. Sci.*, 2010, **3**, 1018.
- 10 V. Artero, M. Chavarot-Kerlidou and M. Fontecave, *Angew. Chem., Int. Ed.*, 2011, **50**, 7238–7266.
- 11 F. Jiao and H. Frei, *Angew. Chem., Int. Ed.*, 2009, **48**, 1841–1844.
- 12 F. Zhang, A. Yamakata, K. Maeda, Y. Moriya, T. Takata, J. Kubota, K. Teshima, S. Oishi and K. Domen, *J. Am. Chem. Soc.*, 2012, **134**, 8348–8351.
- 13 S. Chen, Y. Qi, G. Liu, J. Yang, F. Zhang and C. Li, *Chem. Commun.*, 2014, **50**, 14415–14417.
- 14 S. Chen, S. Shen, G. Liu, Y. Qi, F. Zhang and C. Li, *Angew. Chem., Int. Ed.*, 2015, **54**, 3047–3051.
- 15 G. Zhang, S. Zang and X. Wang, *ACS Catal.*, 2015, **5**, 941–947.
- 16 T. Kanazawa, K. Kato, R. Yamaguchi, T. Uchiyama, D. L. Lu, S. Nozawa, A. Yamakata, Y. Uchimoto and K. Maeda, *ACS Catal.*, 2020, **10**, 4960–4966.
- 17 Y. Nishijima, K. Ueno, Y. Kotake, K. Murakoshi, H. Inoue and H. Misawa, *J. Phys. Chem. Lett.*, 2012, **3**, 1248–1252.
- 18 A. Tanaka, K. Nakanishi, R. Hamada, K. Hashimoto and H. Kominami, *ACS Catal.*, 2013, **3**, 1886–1891.
- 19 M. Kajita, K. Saito, N. Abe, A. Shoji, K. Matsubara, T. Yui and M. Yagi, *Chem. Commun.*, 2014, **50**, 1241–1243.
- 20 K. Maeda, K. Ishimaki, Y. Tokunaga, D. Lu and M. Eguchi, *Angew. Chem., Int. Ed.*, 2016, **55**, 8309–8313.



- 21 K. Maeda, K. Ishimaki, M. Okazaki, T. Kanazawa, D. Lu, S. Nozawa, H. Kato and M. Kakihana, *ACS Appl. Mater. Interfaces*, 2017, **9**, 6114–6122.
- 22 M. Okazaki, Y. Wang, T. Yokoi and K. Maeda, *J. Phys. Chem. C*, 2019, **123**, 10429–10434.
- 23 H. Tanaka, T. Uchiyama, N. Kawakami, M. Okazaki, Y. Uchimoto and K. Maeda, *ACS Appl. Mater. Interfaces*, 2020, **12**, 9219–9225.
- 24 A. Harriman, I. J. Pickering, J. M. Thomas and P. A. Christensen, *J. Chem. Soc., Faraday Trans. 1*, 1988, **84**, 2795–2806.
- 25 M. W. Kanan and D. G. Nocera, *Science*, 2008, **321**, 1072–1075.
- 26 G. L. Elizarova, L. G. Matvienko, N. V. Lozhkina, V. N. Parmon and K. I. Zamaraev, *React. Kinet. Catal. Lett.*, 1981, **16**, 191–194.
- 27 P. M. Scop, *Phys. Rev.*, 1965, **139**, A934–A940.
- 28 P. Wang, B. Huang, X. Qin, X. Zhang, Y. Dai, J. Wei and M. H. Whangbo, *Angew. Chem., Int. Ed.*, 2008, **47**, 7931–7933.
- 29 A. Currao, V. R. Reddy and G. Calzaferri, *ChemPhysChem*, 2004, **5**, 720–724.
- 30 L. Han, P. Wang, C. Zhu, Y. Zhai and S. Dong, *Nanoscale*, 2011, **3**, 2931–2935.
- 31 K. Maeda, M. Higashi, D. Lu, R. Abe and K. Domen, *J. Am. Chem. Soc.*, 2010, **132**, 5858–5868.
- 32 A. Kasahara, K. Nukumizu, G. Hitoki, T. Takata, J. N. Kondo, M. Hara, H. Kobayashi and K. Domen, *J. Phys. Chem. A*, 2002, **106**, 6750–6753.
- 33 D. R. Lide, *CRC Handbook of Chemistry and Physics*, CRC Press, 84th edn, 2003.
- 34 A. Ono, R. Matsumoto and N. Yamaguchi, *Trans. Iron Steel Inst. Jpn.*, 1982, **22**, 121–125.
- 35 A. Selmani, J. Lutzenkirchen, N. Kallay and T. Preocanin, *J. Phys.: Condens. Matter*, 2014, **26**, 244104.
- 36 R. Kuriki, K. Sekizawa, O. Ishitani and K. Maeda, *Angew. Chem., Int. Ed.*, 2015, **54**, 2406–2409.
- 37 C. Cometto, R. Kuriki, L. Chen, K. Maeda, T. C. Lau, O. Ishitani and M. Robert, *J. Am. Chem. Soc.*, 2018, **140**, 7437–7440.

